



# Model study of the geotechnical behavior of a single pile under torsional load in contaminated sand

Nada Osama Ramadan<sup>1</sup> · Ahmed Mohamed Nasr<sup>2</sup> · Waseim Ragab Azzam<sup>2</sup>

Received: 18 December 2022 / Accepted: 9 November 2023 / Published online: 28 November 2023  
© Saudi Society for Geosciences and Springer Nature Switzerland AG 2023

## Abstract

In varieties of coastal soil, deep foundations, particularly pile foundations, are used because the soil in these areas may be subjected to numerous factors that change the engineering properties of the soil, such as oil pollution. The pile foundations might be vulnerable to torsional stresses from eccentric, horizontal loads brought on by winds, earthquakes, shipwrecks, and waves, in addition to the loads carried by supported superstructures. In this laboratory investigation, tests have been carried out to investigate the behavior of piles under torsional load (T) and combined torsional-vertical load (T → V) in contaminated sandy soils. Additionally, investigations examined how the  $L_p/D_p$  ratio, relative density ( $D_r$ ), and depth of the contaminated layer ( $L_c$ ) affect their maximum torsional bearing capacity, which was discussed in detail. According to the findings, oil contamination significantly decreased pile response, and it also demonstrated that independent load differs significantly from combined load, in which the ultimate vertical bearing capacity of the piles in  $D_r = 30\%$  installed in contaminated sand under pre-applied torque T → V loading at  $L_c/L_p = 1$  decreases by 3.3, 3.9, and 5.1% for  $L_p/D_p$  20, 16.67, and 13.3, respectively. These results show that the pile design must take into account the amalgamated loading of contaminated sand.

**Keywords** Contaminated sand · Pile foundation · Combined torsional-vertical load · Torsional load

## Introduction

Many factors lead to changes in the engineering, physical, and chemical properties of the soils in marine and coastal environments, such as oil spills, the impact of ships, the collision of waves, and marine turbines. In this case, shallow foundations will be insufficient due to the severity of weak soil, so deep foundations such as piles are used. Piling foundations are widely used, mainly in large structures such as offshore platforms, wind turbines, tall buildings, bridges, and railways. They help strengthen weak soils

and withstand torsional loads resulting from wind loads, earthquakes, ship impacts, and wave collisions, as well as vertical loads transmitted by superstructures (Azzam 2015, and Basack and Nimbalkar 2017). Also, piles are used to transfer torsion loads to the lower layers, which are supported by a fixed safety factor. When the depth increases, the torque gradually decreases, indicating the torsional pile resistance must be overcome before the torsional load can be transferred to the surrounding soil (Zou et al 2021). In the previous literature, there were not many studies that dealt with the behavior of piles under single torsional loads or combined loads (vertical and torsional loads) in contaminated sand. Several studies have been performed on clean soils with vertical loading in standardized soils (Guo and Randolph 1997 and Guo 2000) and contaminated soils (Dhatrak et al. 2017 and Mohammadi et al. 2018). There are many theories methods, such as the elasticity theory (Poulos and Davis 1968) and the load transfer method (Guo and Randolph 1997). Furthermore, numerical methods such as the boundary element method (Chow 1985), the finite element method (Basack and Sen 2014), and the finite difference method (Li and Stuedlein 2018). Recently, a direct and effective method

Responsible Editor: Zeynal Abiddin Erguler

✉ Nada Osama Ramadan  
Nada152184@f-eng.tanta.edu.eg

Ahmed Mohamed Nasr  
ahmed.nasr@f-eng.tanta.edu.eg

Waseim Ragab Azzam  
waseim.azzam@f-eng.tanta.edu.eg

<sup>1</sup> Structural Engineering Department, Faculty of Engineering, Tanta University, Tanta, Egypt

<sup>2</sup> Faculty of Engineering, Tanta University, Tanta, Egypt

has been planned to overcome the nonlinear response of single piles under the influence of torsional loads (Nghiem and Chang 2019). In addition to these studies, three types of torsional tests were conducted on single piles, as follows: (1): small model tests such as Poulos (1975), Dutt and O'Neill (1983), Randolph (1983), Tawfiq (2000), and Zou et al. (2021); (2) typical tests of multiple centrifuges such as Bizaliele (1992), Laue and Sonntag (1998), McVay et al. (2003b), McVay and Hu (2003a), and Zhang and Kong (2006); (3) tests on full-scale driven piles and drilled shafts such as Stoll (1972), Tawfiq (2000), McVay et al. (2014), Thiyyakkandi et al. (2016), and Li et al. (2017). Among those tests, Stoll (1972) performed a large-scale torsion test on two steel columns filled with concrete. Both shafts' torsional resistance increased as shaft rotation increased, until failure at about  $3.2^\circ$ . Poulos' charts (1975) provided a valuable tool for engineers to estimate the torsion flexibility of pile shafts and optimize their design for different applications. This approach allowed for the analysis of torsional behavior in various soil conditions, and a continuum mechanics technique was used to account for the soil-pile interaction. Dutt (1976) and Dutt and O'Neill (1983) were the first to study the torsional bearing capacity of a pile installed in sand. Their research's objective was to understand how the relative density of the sand and the method of installing the piles affected the ability of torsion for circular and square piles (Zhang and Kong 2006). They found that the critical rotation angle was determined by the maximum torsional moment that the tube could withstand before failure. This information is crucial for understanding the accurately assessing response of tubes under torsional loading conditions. These results did not agree with those reported by Dutt and O'Neill (1983) and Tawfik (2000). Zou et al. (2021) provided testing on a single aluminum pile to study the torsional response of multi-layer soil and the effect of soil type and properties on torsion and torsion angle. Tests were carried out under independent vertical loads (V), independent torsional loads (T), and combined vertical and torsional loads (V-T). It was discovered that the research cited in the literature evaluated the torsional behavior of a single pile under various circumstances. The behavior of piles under torsion in clean soil was also the subject of several studies and tests. However, it has not been found to fully study the impact of soil contamination with both torsional and vertical stresses on contaminated sand. As a result, experiments will be carried out in this research to ascertain the behavior of the piles under combined loads in polluted sandy soil. For the sake of comparison, the experiments were conducted on clean sandy soils. There were three alternative pile lengths and various densities employed to shed light on the induced torsional loads at the different investigated parameters.

**Table 1** Dimensions of model piles

Pile number	Pile diameter, D (mm)	Total length, L (mm)	Embedment depth, L <sub>p</sub> (mm)	Slenderness ratio, L <sub>p</sub> /D <sub>p</sub>
1	30	700	600	20
2	30	600	500	16.67
3	30	500	400	13.3

**Table 2** Properties of model piles

Properties	Pile diameter, D (mm)	Pile thickness, t (mm)	Pile density, $\rho$ (kg/m <sup>3</sup> )	Pile Young's modulus E <sub>p</sub> (GPA)	Pile material
Model	30	1.5	7850	210	steel

## Research significance

Laboratory experiments have been conducted, to determine the behavior of the pile under independent vertical load (V), independent torsion load (T), and amalgamated loads (T → V) in the contaminated sandy soil at different parameters. The results were compared with the results of clean sandy soil.

## Mode test arrangement

### Model piles

In this laboratory study, three hollow steel rough piles with closed ends were utilized, as clarified in Table 1. The maximum shear stress mobilized through rough surfaces was determined to be slightly scale effect dependent based on a series of torsional pile experiments in the sand (Garnier and Konig 1998). A 30 mm pile diameter model was used in this research to ensure that the sand grain size distribution used in this study, where the pile diameter (D<sub>p</sub>) means sand grain size (D<sub>50</sub>), is more than 30 (Franke and Muth 1985). The model pile was designed with lengths of 700, 600, and 500 mm. The ratios of pile length to pile diameter (L<sub>p</sub>/D<sub>p</sub>) utilized were 20, 16.67, and 13.3. The pile thickness is 1.5 mm to fulfill this condition and provide torsional resistance. Table 2 provides a summary of the model pile's properties.

### Test tank

A rectangular steel tank has been used in laboratory testing. According to Leblanc et al. (2010), the tank’s dimensions were set at 80 \* 60 \* 60 cm, where the distance between the substrate and the tank wall should be larger than 8D–10D. This was based on the measurements of the substrate, which were used to determine the effective squeezing area of the adjacent soil. Additionally, according to Garnier et al. (2007), Bolton et al. (1999), and Craig and Sabagh (1994), the distance between the bottom of the pile and the bottom of the tank is greater than 5 D (where D is the diameter of the pile). This prevents bending of the tank wall, which would otherwise cause subsidence of effective vertical pressure with depth, which is dependent on the ratio between the reservoir’s height and width (Garnier 2001; Nasr and Azzam 2017). The thickness of the tank wall was fixed at 3 mm to avoid any lateral deformation on the tank sides. Figure 1 shows an illustration of the configuration of the device.

### Material and methods

#### Clean sand

The laboratory tests were carried out on dry sand. According to the Unified Soil Classification System (ASTM

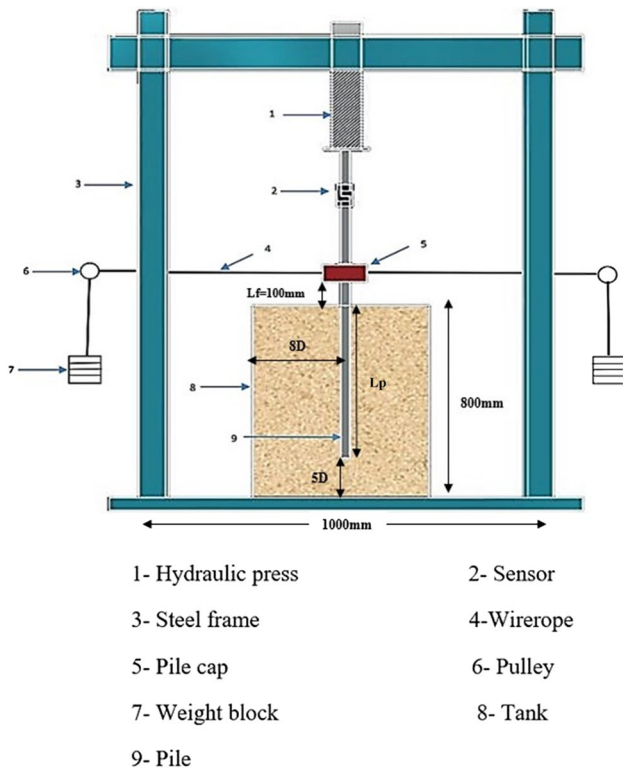


Fig. 1 A graphic illustrating the configuration of the device (without scale)

2010), the sand utilized in this study is classified as poorly graded sand (SP). The jar technique was used to calculate the soil particles’ specific gravity (Gs) (Sakr et al 2016 and 2020). An average value of (Gs) was obtained from five laboratory tests to be 2.65. The examined sand’s minimum and maximum dry unit weights were determined to be 16.57 kN/m<sup>3</sup> and 18.60 kN/m<sup>3</sup>, respectively. While the equivalent values of the minimum and maximum void ratios were 0.42 and 0.59, respectively. Figure 2 clarifies the sand’s utilized particle size distribution curve. According to Nasr (2014) and Sakr et al. (2020), the circular grains of the sand used in the test helped to reduce any possible friction that could have existed between the soil and the steel box walls. The sand was positioned to obtain two relative densities: the loose condition (Dr = 30%) and the dense condition (Dr = 80%). For loose and dense sand conditions, experiments were carried out at two different unit weights: 16.60 kN/m<sup>3</sup> and 18.20 kN/m<sup>3</sup>, respectively. The shear strength parameters of sand in loose and dense states were obtained using direct shear testing (Nasr 2014 and Sakr et al 2020). For the loose and dense states, the values of friction angles (ϕ) were found to be 35° and 40°, respectively. Table 3 provides a summary of the other characteristics of the examined sand.

#### Oil properties and contaminated sand installation

The laboratory tests in this study were conducted using heavy motor oil. The Misr Petroleum Company in Tanta provided the heavy motor oil that was purchased. Tests were carried out at a temperature of 25°, and the characteristics are shown in Table 4. The oil’s chemical composition was made up of a combination of aromatic hydrocarbons and

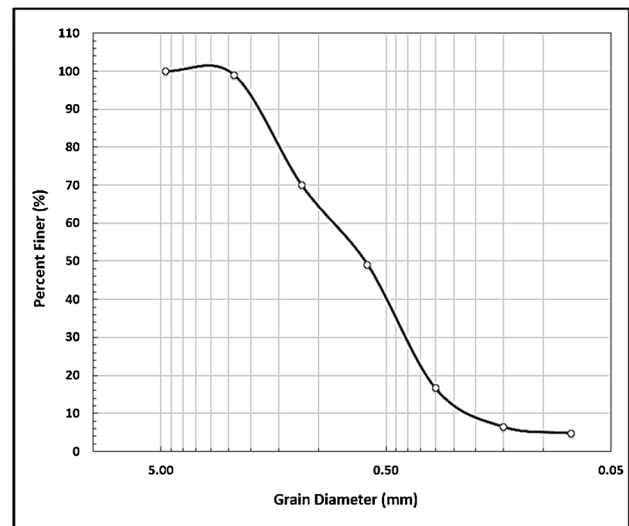


Fig. 2 The utilized sand’s particle-size distribution curve



to the pile's toe initially. To get the required relative density, the weight of the dirt poured into each layer was calculated until all layers had the same density. For contaminated sand, the loading layer was first filled to a depth of 20 cm, and then the surrounding soil was subsequently filled with the contaminated layer at various depths. Each layer of sandy dirt was then compacted using a 4.5-kg iron plate. The findings in Fig. 3 display that until the oil content percentage reaches 6%, the torsion capacity decreases dramatically with an increase in the oil content percentage; after this percentage, the torsion capacity decreases slightly. This is because the amount of oil in the soil is increasing, which increases the lubricating effect on soil particles and reduces the shear strength of sandy soil. Additionally, it was discovered that when the oil content (O.C.) increased from 0 to 2%, the friction angle value ( $\phi$ ) significantly decreased. However, the

reduction rate of friction angle ( $\phi$ ) decreased at a negligible rate at oil content greater than 4% (Nasr 2009 and 2013), Nasr and Krishna Rao (2016) and Abdelhalim et al (2020), so the current study depends on an oil percentage of 6%.

### System for loading

According to Fig. 1, the loading system has been designed to measure vertical (V), torsional (T), and combined loads (vertical and torsional loads). A vertical load was applied using a hydraulic piston system. In contrast, blocks hung by a rigid-flexible wire rope strung on a steel pulley secured to the pile cap were used to apply the torsion force (assuming the wire is inextensible). Additionally, by adjusting the height of the torsional load on the frame, it is possible to make the wire rope between the pulley and the pile cap horizontal. While loading, the loading direction should be taken into account, so this device can maintain the loading direction. The torsional load on the pile head was calculated using the equation  $T_u = \mu mgL_t$ , where  $\mu$ , coefficient of pulley friction;  $m$ , block weight;  $g$ , gravity acceleration; and  $L_t$ , torsion arm. The torsional arm  $L_t$  and pulley friction coefficients have been determined to be 0.8 and 75 mm, respectively. An indicator was placed on the pile cap whose center matches the center of the pile in order to determine the angle of torsion of the pile. A sensor was placed to detect the vertical pressure on the pile head, and two dial gauges were placed on the pile cap to record the vertical displacement that occurred.

### Testing program and studied parameters

Three pile lengths are subjected to the experiments utilizing the sustainable load technique to verify the piles' static response in both clean and oil-contaminated sand, as well as loose and dense sand (Zhang and Kong 2006; Dutt 1976; Dutt and O'Neill 1983; Zhang and Kong 2006; and Zou et al 2021). Blocks are placed sideways at a loading rate of  $0.2^\circ$  per second (Zhang and Kong 2006; Zou et al 2021). According to Zhang and Kong (2006) and Zou et al. (2021), additional weight was applied to the pile until significant lateral displacements or rotations of an angle had occurred. The loading direction remains constant during the experiment, and the protractor indicator readings are recorded with adequate time between each further loading (Nasr 2014; Sakr et al 2016 and 2020). Results are expressed as applied torsion load (T) and rotation angle ( $\theta$ ). Model experimental tests were conducted on piles in contaminated sand at various thinness ratios ( $L_p/D_p$ ), where  $L_p$  is the pile's embedded length and  $D_p$  is its diameter. These tests were conducted because the current investigation is limited in scope, and there are few studies on torsional testing of piles in contaminated sand. The studied  $L_p/D_p$  values are 20, 16.67, and 13.3. Various relative densities between 30

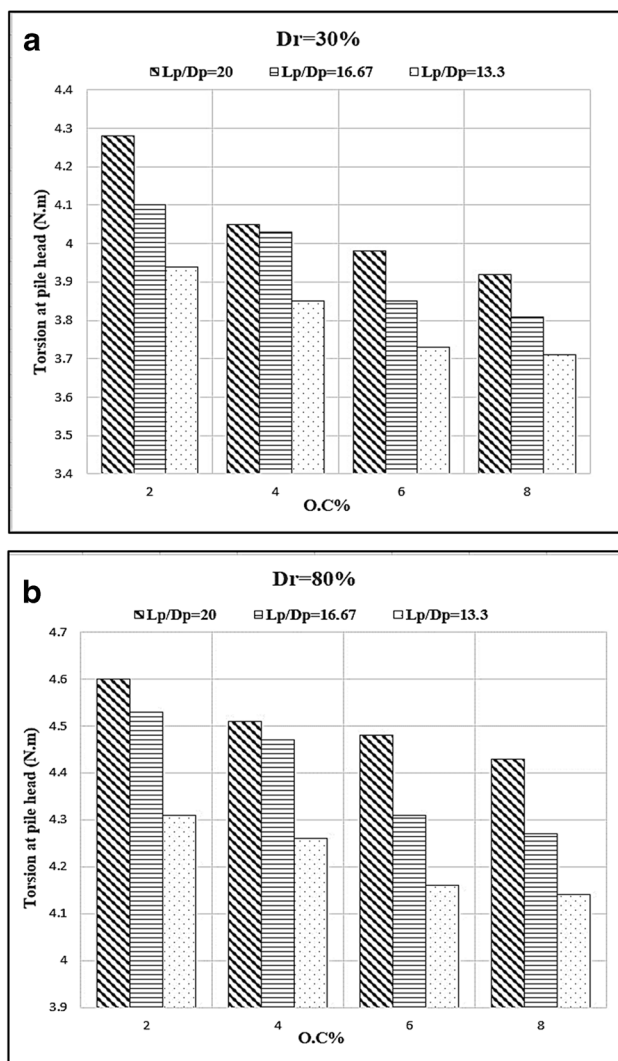


**Fig. 3** Variation of the maximum torsion load with different oil contents (O.C%) at  $L_c/L_p = 1$

and 80% were used for the testing. To assess how piles in contaminated sand will behave with regard to torsion capacity under various parameters, piles in clean sand were tested as a comparison. These factors were the thinness ratio ( $L_p/D_p$ ), the relative density of sand ( $Dr\%$ ), and the thickness of the contaminated layers ( $L_c$ ). At a constant oil concentration of 6%, all experiments were conducted. In Table 6, the experimental testing schedule is described in full. From the given data from these tests, it can be calculated that torsion along pile ( $T_i$ ) (Wang et al. 2020) and rotation angle along pile ( $\theta_z$ ) (Basack et al. 2011) are employed and described as:

$$T_i = T - \sum_{i=0}^{n-1} 0.5\pi\tau_i(i)D^2h \quad (1)$$

where  $T_i$ , torque at depth  $i$ ;  $T$ , torsion load;  $\tau_i$ , vertical frictional resistance of the pile at depth  $i$ ;  $D$ , diameter of the pile;  $h$ , length of pile unit.

$$\theta_z = \int_0^L \int_0^L \frac{D^2}{2J_p G_p} \tau_z d_z d_z \quad (2)$$

where  $\theta_z$ , rotation angle at depth  $z$ ;  $D$ , diameter of the pile;  $G_p$ , shear modulus;  $J_p$ , polar moment of inertia of pile section;  $\tau_i$ , vertical frictional resistance of the pile at depth  $z$ .

## Results with discussion

### Behavior of pile under independent torsion load

Torsion is commonly generated by the eccentric divergence of the load; consequently, the torsion load must be taken into account while constructing structures, especially pile foundations. In the current study, the findings of torsional testing have been reported and thoroughly explained. According to previous investigations, the following criteria were suggested for determining the ultimate load of the torsion of the piles: First (Stoll 1972; Guo and Zou 2018), the load value that coincides with the observed inflection point of the curve ( $T-\theta$ ) was used to define the maximum torsion bearing capacity; second (Georgiadis and Saflekou 1990; and Li and Stuedlein

2018), the maximum torsional load of the piles is the force at which the curve becomes linear; and third (Zhang and Kong 2006), the maximum torsion angle of the piles is defined by the value of the intersection of the linear line by the empirical formula and the curve ( $T-\theta$ ). The findings of the curve ( $T-\theta$ ) in this investigation indicated a definite inflection point; therefore, the first technique is appropriate for this study (Stoll 1972; Guo and Zou 2018). The performance of the pile may be assessed according to the test results obtained from the ( $T-\theta$ ) curves for different values of the relative density of the sand ( $Dr=30$  and 80%), the thickness of the contaminated layers ( $L_c$ ), and the thinness ratio ( $L_p/D_p$ ), as shown in Figs. 4 and 5. To support the analysis, the results are also presented in Table 7. According to Fig. 4a, it can be seen that the ultimate torsional load in clean sand at relative densities of  $Dr=30$  and 80% for  $L_p/D_p=16.67$  is 4.26 and 4.77 N.m, respectively. Figure 4 b, c, and d demonstrate the behavior of piles subjected to torsion loads in oil-contaminated sand at relative densities ( $Dr=30$  and 80%) with stiffness ratios  $L_p/D_p=16.67$  in the case of  $L_c/L_p=0.4, 0.8$ , and 1. The maximum torsional load in contaminated loose sandy soil was determined to be 3.93, 3.88, and 3.85 N.m., respectively, while in contaminated dense sandy soil, these values were found to be 4.42, 4.35, and 4.31 N.m at  $L_c/L_p=0.4, 0.8$ , and 1, respectively. Figure 5 clarifies the relationship between the applied torsional load and torsion twist angle of the piles set up in contaminated sand at relative densities ( $Dr=30$ , and 80%) with  $L_p/D_p=20, 16.67$ , and 13.3 and  $L_c/L_p=1$ . The torsional load at  $1^\circ$  was found to be 25%, 31%, and 39% of the ultimate torsion load for single piles at  $Dr=30\%$ , respectively, while, in the case of  $Dr=80\%$ , these values reached 33, 43, and 52% in the same order. It is clear that the maximum torsional load rises for a given torsion angle value when the angle of the sand's shearing resistance rises. This is consistent with the findings of Dutt (1976), Dutt and O'Neill (1983), and Zhang and Kong (2006). Figures 4d and 5 a and b show that the curve of ( $T-\theta$ ) is linear up to 35, 31, and 29% of the maximum torsion when  $L_p/D_p=20, 16.67$ , and 13.3 and  $L_c/L_p=1$ , respectively, at relative density  $Dr=30\%$ , whereas these values were discovered to be 17, 14, and 10% of the maximum torsion at relative density

**Table 6** Parameters for testing laboratory model program

Series	Constant parameters	Variable parameters
I	$L_p/D_p=20$	$L_c/L_p=0, 0.33, 0.67, 1$ , and 1.16 at $Dr=30\%$ , and O.C=6%
II		$L_c/L_p=0, 0.33, 0.67, 1$ , and 1.16 at $Dr=80\%$ , and O.C=6%
III	$L_p/D_p=16.67$	$L_c/L_p=0, 0.4, 0.8, 1$ , and 1.2 at $Dr=30\%$ , and O.C=6%
IV		$L_c/L_p=0, 0.4, 0.8, 1$ , and 1.2 at $Dr=80\%$ , and O.C=6%
V	$L_p/D_p=13.3$	$L_c/L_p=0, 0.5, 0.75, 1$ , and 1.25 at $Dr=30\%$ , and O.C=6%
VI		$L_c/L_p=0, 0.5, 0.75, 1$ , and 1.25 at $Dr=80\%$ , and O.C=6%

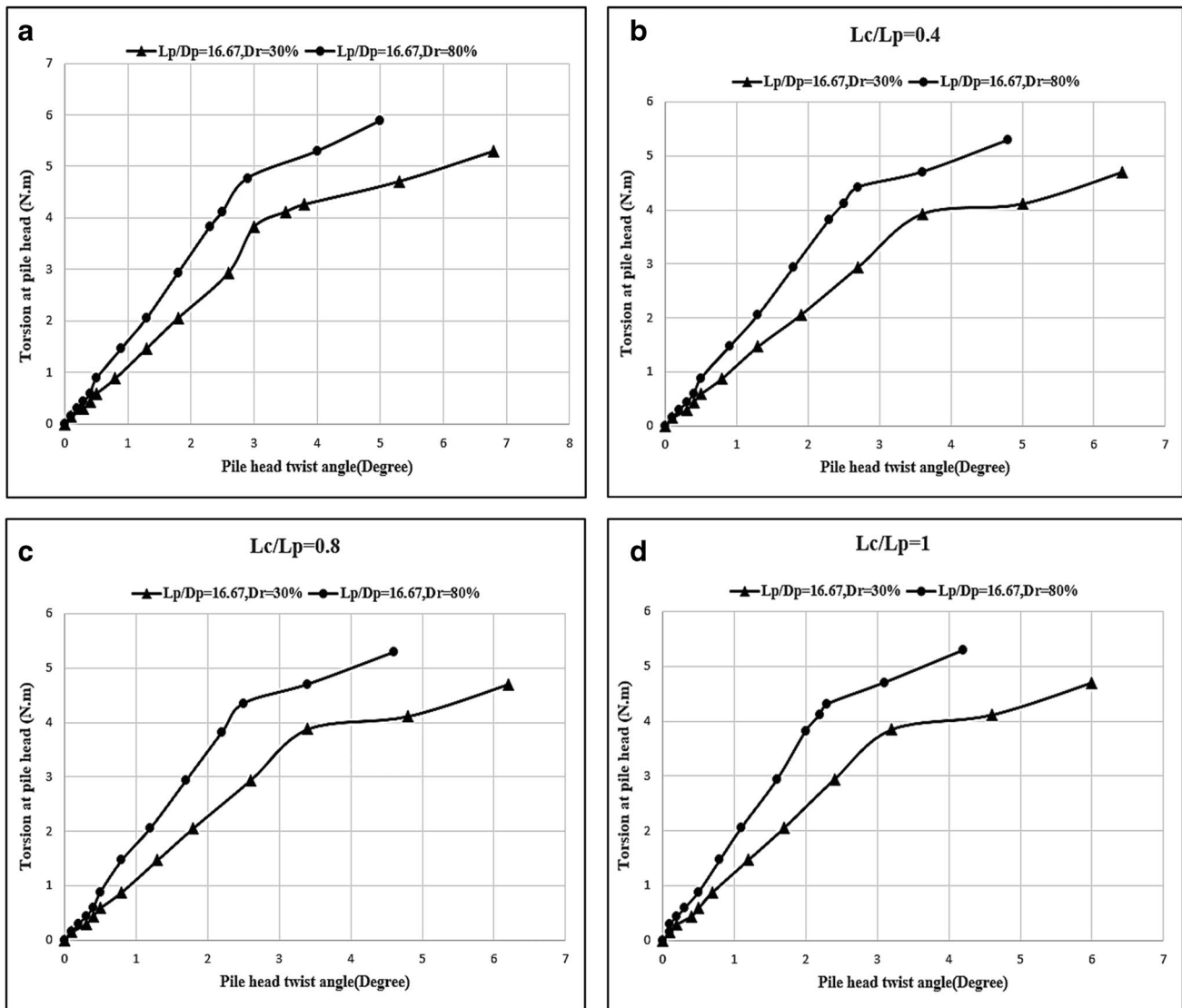


**Fig. 4** Relationship between the applied torsional load and twist angle, **a** clean sand, **b** contaminated sand at  $L_c/L_p=0.4$ , **c** contaminated sand at  $L_c/L_p=0.8$ , **d** contaminated sand at  $L_c/L_p=1$

$D_r = 80\%$  at the same order. The findings demonstrated that the torsional angle did not rise at the same rate as the torque when the torsional load was raised. As a result, the torsional load became very sensitive. Additionally, when the applied torsional load was less than the value of the load corresponding to the torsion angle of  $1^\circ$ , the curves were near each other, indicating that torsion is somewhat impacted by the bearing layer.

**Behavior of pile under independent vertical load**

Figures 6 and 7 show a typical relationship of the vertical load against the settlement curve for piles in clean and contaminated sandy soil, installed in loose and dense sand

conditions. According to previous works of literature, the following criteria were suggested for determining the ultimate vertical load: First (Guo and Zou 2018), the piles’ maximum vertical bearing capacity is the number that corresponds to the curve’s apparent inflection point (P-S); second (Poulos and Davis 1980), the ultimate vertical load-bearing capability of the piles is equal to the amount that corresponds to the ultimate vertical displacement; and third (Nabil 2001), at the intersection of the first tangent, the ultimate vertical load value is determined using the slope tangent technique. In this study, the ultimate vertical load was determined using the second method (Poulos and Davis 1980) because the findings of the curve (P-S) revealed no obvious inflection point, and the value corresponds to 10% D with a value of

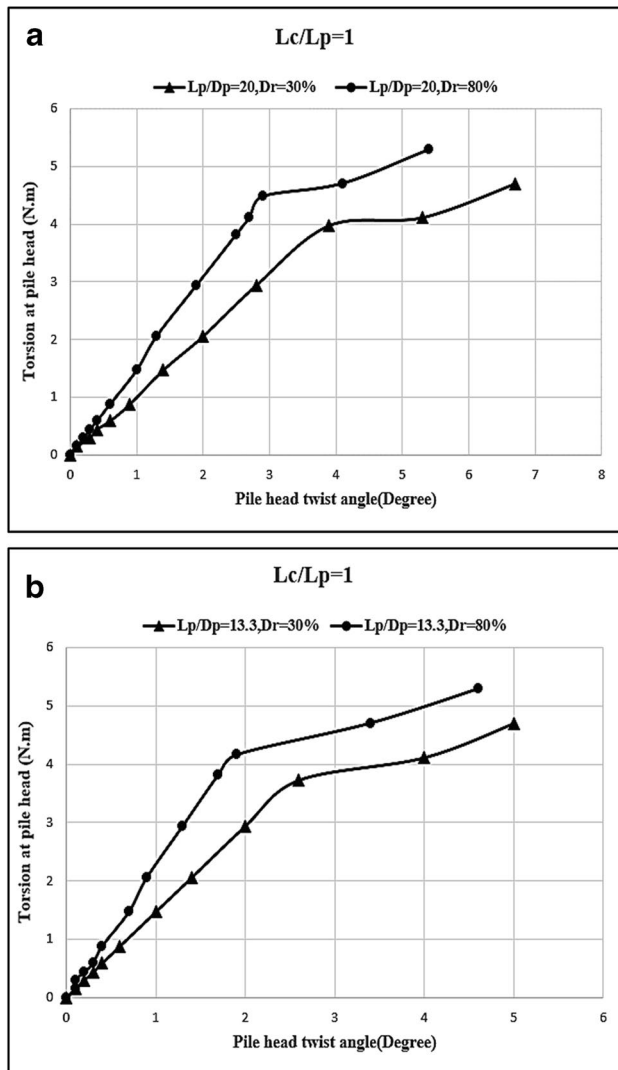


**Fig. 5** Relationship between the applied torsional load and torsion twist angle in contaminated sand at  $L_c/L_p=1$ , **a**  $L_p/D_p=20$ , **b**  $L_p/D_p=13.3$

3 mm. As can be seen from Fig. 6a, the ultimate vertical load in clean sand at relative densities ( $D_r=30$  and  $80\%$ ) in the case of  $L_p/D_p=16.67$  is 2500 and 3300 N, respectively. Figures 6 b, c, and d demonstrate the behavior of piles subjected to vertical loads in oil-contaminated sand at relative densities ( $D_r=30$  and  $80\%$ ) with stiffness ratios  $L_p/D_p=16.67$  in the case of  $L_c/L_p=0.4, 0.8$ , and  $1$ . The maximum vertical load in contaminated sand soil was found to be 2300, 2240, and 2210 N at  $D_r=30\%$ , respectively, while in the case of  $D_r=80\%$ , these values were found to be 3050, 2760, and 2650 N at  $L_c/L_p=0.4, 0.8$ , and  $1$ , respectively. This is in agreement with the findings of Zou et al. (2021). It was clarified from Fig. 7 a and b, that the curve of (P-S) is linear until 18, 29, and 50% of the maximum vertical load; after that, the relationship becomes linear in the case of  $L_p/D_p=20, 16.67$ , and  $13.3$  and  $L_c/L_p=1$  at relative density  $D_r=30\%$ , respectively, while these values were found to be 12, 20, and 33% of the maximum vertical load; after that, the relationship becomes linear at relative density  $D_r=80\%$  at the same order. As a result, it is concluded that the bearing layer has a greater impact on the eventual vertical bearing capacity of a pile than the surrounding soil.

**Table 7** Maximum torque (N.m.) in dense and loose sand

Soil	$L_c/L_p$	Ultimate torsion (N.m) at $D_r=30\%$	Ultimate torsion (N.m) at $D_r=80\%$
$L_p/D_p=20$	0	4.42	4.97
	0.33	4.08	4.62
	0.67	4.03	4.55
	1	3.98	4.48
$L_p/D_p=16.67$	0	4.26	4.77
	0.4	3.93	4.42
	0.8	3.88	4.35
	1	3.85	4.31
$L_p/D_p=13.3$	0	4.11	4.57
	0.5	3.78	4.23
	0.75	3.75	4.19
	1	3.73	4.16

**Behavior of pile under amalgamated Load ( $T \rightarrow V$ )**

Figures 8, 9, and 10 show the response of the pile for vertical load under constant various torsion loads ( $T = 1/3 T_u, 2/3 T_u$ , and  $T_u$ ) in clean and contaminated sand, set up in loose and dense sand circumstances. Also, the findings are briefed as illustrated in Table 8 to be justified. From the figures, it can be observed that the slope of the (P-S) curves does not vary with increasing constant torsional loads. As a result, the maximum settlement under various torsional levels of the load is the same, equivalent to 3 mm. As can be shown from Figs. 8 a and b, the ultimate vertical load under combined load at constant torsional load ( $T = 1/3 T_u$ ) in clean sand at relative densities ( $D_r=30$  and  $80\%$ ) was found to be reduced by 1.5 and 2% than piles under independent vertical load in the case of  $L_p/D_p=16.67$ , respectively, while at constant torsional load ( $T = 2/3 T_u$ ), these values were found to be reduced by 2.5 and 2.1% at relative densities  $D_r=30$  and  $80\%$ , respectively. Figure 9 a, b, and c explain the ultimate vertical load under combined load at constant torsional load ( $T = 1/3 T_u$ ) in the case of  $L_p/D_p=16.67$  and  $L_c/L_p=0.4, 0.8$ , and  $1$ . The ultimate vertical load under combined load in contaminated sand was reduced by 1.9, 1.5, and 1.3% to piles under independent vertical load at  $D_r=30\%$ , respectively, while in the case of  $D_r=80\%$ , these values

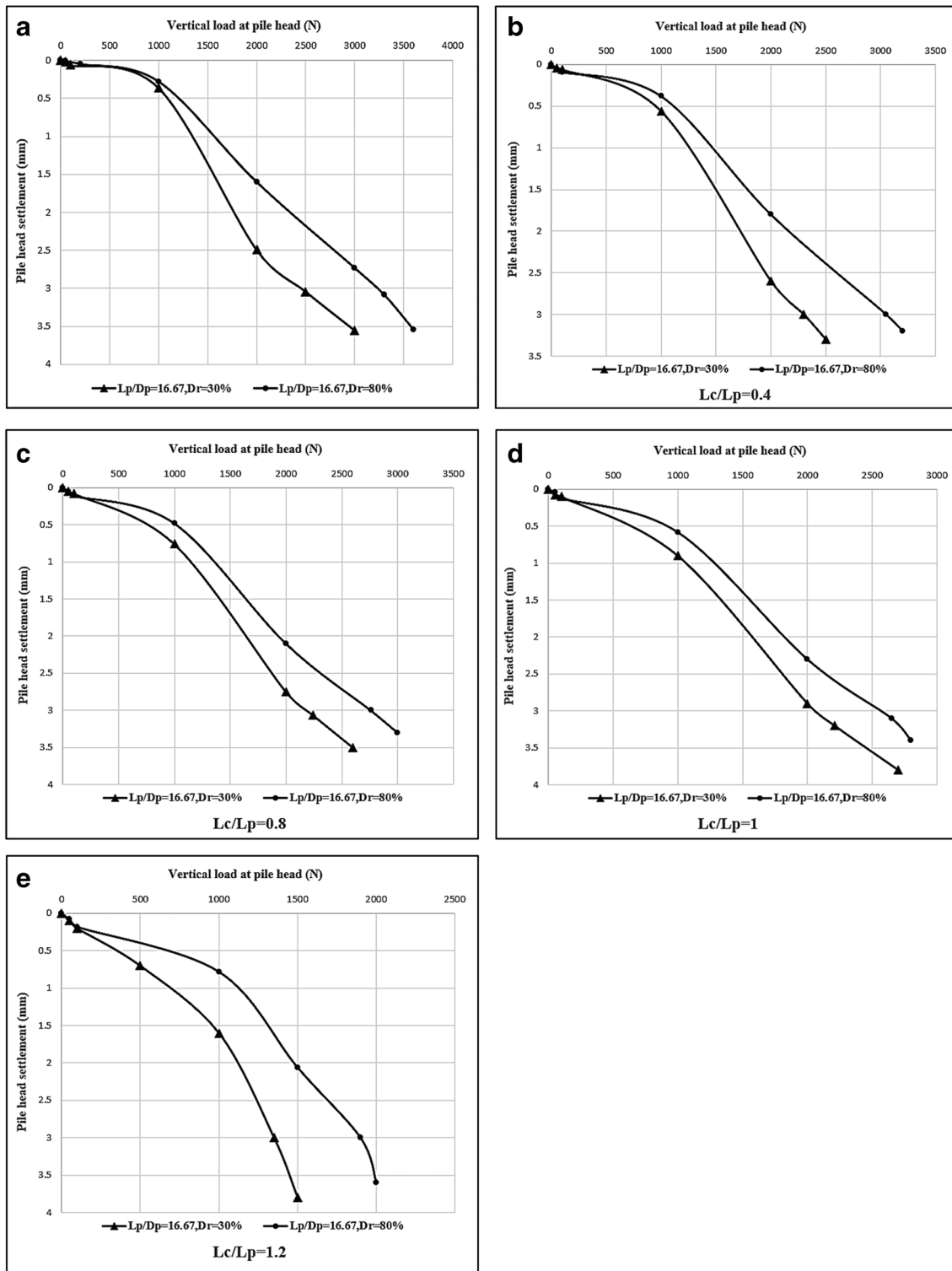


**Fig. 6** Relationship between the applied vertical load and settlement in contaminated sand at  $L_p/D_p = 16.67$ , **a** clean sand, **b** contaminated sand at  $L_c/L_p = 0.4$ , **c** contaminated sand at  $L_c/L_p = 0.8$ , **d** contaminated sand at  $L_c/L_p = 1$ , **e** contaminated sand at  $L_c/L_p = 1.2$

were found to reach 1.3, 1.4, and 1.5% in the same order. In the case of  $L_p/D_p = 16.67$  and  $L_c/L_p = 0.4, 0.8$ , and 1 at constant torsional load ( $T = 2/3T_u$ ). It was found that the

ultimate vertical load under combined load was reduced by 2.4, 2.5, and 2.6% compared to piles under independent vertical load at  $D_r = 30\%$ , while these values reached

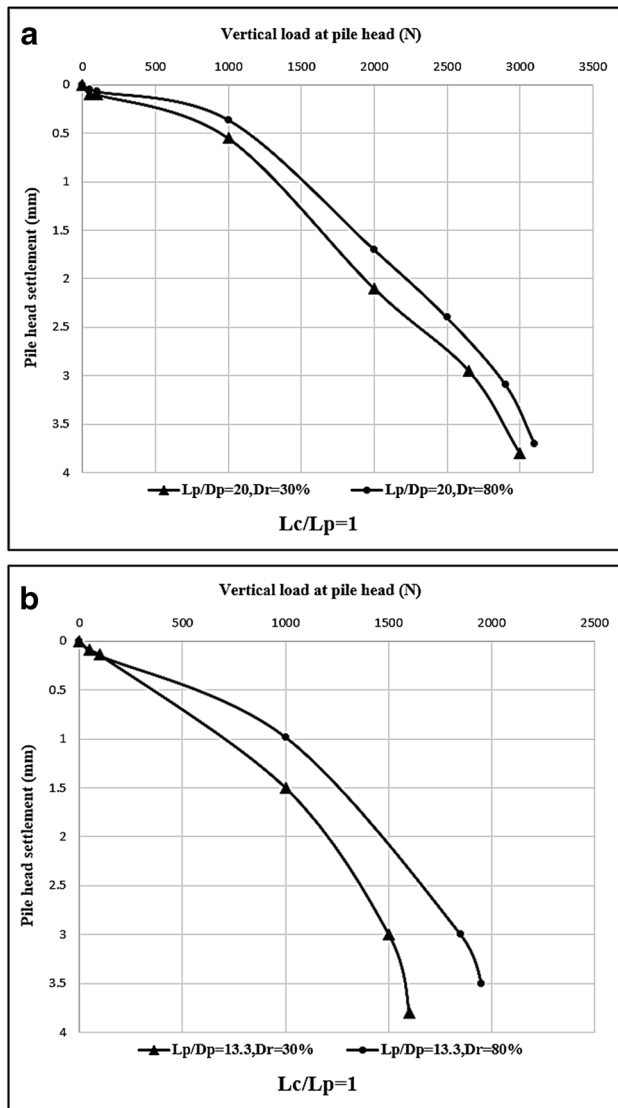


**Fig. 7** Relationship between the applied vertical load and settlement in contaminated sand at  $L_c/L_p = 1$ , **a**  $L_p/D_p = 20$ , **b**  $L_p/D_p = 13.3$

2.1, 2.2, and 2.4% at  $D_r = 80\%$  in the same order. From Fig. 10 a and b, in the case of  $L_p/D_p = 20, 16.67$ , and  $13.3$  and  $L_c/L_p = 1$  at constant torsional load ( $T = 2/3T_u$ ); when compared to piles under independent vertical loads at  $D_r = 30\%$ , it was discovered that the ultimate vertical load under combined loads decreased by 3.6, 3.4, and 3.1%, while these percentages were reached (3.8, 3.6, and 3.5%) at  $D_r = 80\%$  in the same order. From the findings, the increase in the ratio of length to diameter ( $L_p/D_p$ ) for the pile leads to a decrease in the vertical bearing capacity of the piles under the compound loading. From Fig. 11, the settlement at constant torsional load ( $T = 1/3T_u$ ) and the same vertical load, in the cases of  $L_p/D_p = 16.67$  and  $L_c/L_p = 1$ , was found to be 12 and 18% higher than the settlement at no torsional load ( $T = 0$  N.m.) at  $D_r = 30$

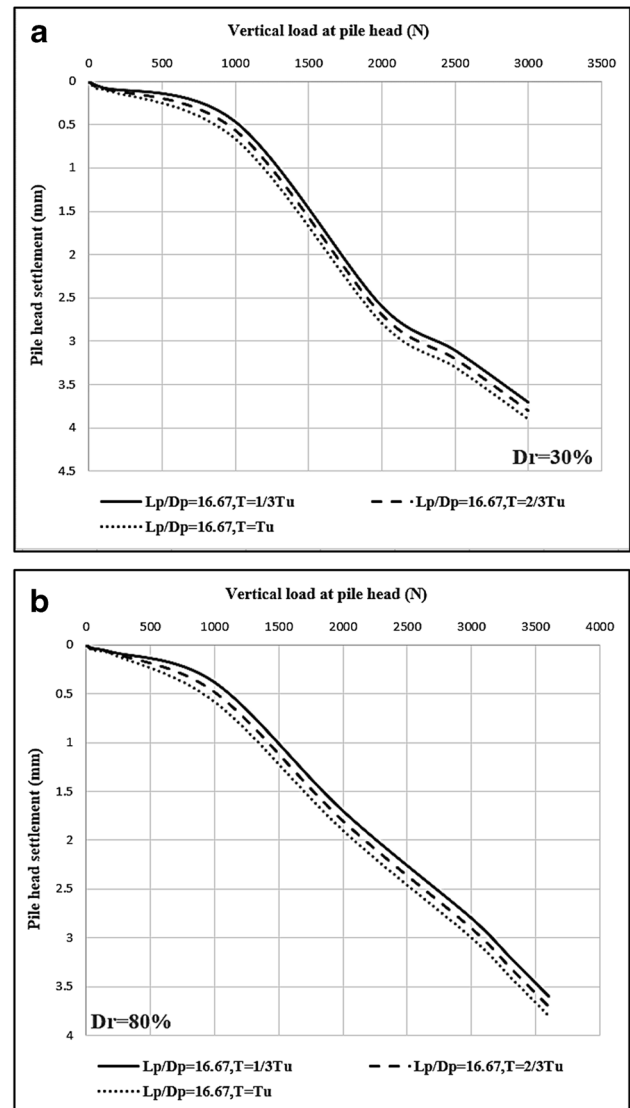


**Fig. 8** Relationship between the applied vertical load and settlement under pre-applied torsion load in clean sand at  $L_p/D_p = 16.67$ , **a** loose sand, **b** dense sand

and 80%, respectively, while at constant torsional load ( $T = 2/3 T_u$ ) and the same vertical load, the settlement was increased by 25 and 35% than the settlement at no torsional load ( $T = 0$  N.m.) in the cases of  $L_p/D_p = 16.67$  and  $L_c/L_p = 1$ , at  $D_r = 30$  and  $80\%$ , respectively. It can be concluded from the analysis that the pile's P-S curves at  $T = 1/3 T_u$  and  $T = 0$  N.m are near. Nevertheless, while the constant torsional load increases to  $T = 2/3 T_u$ , the pile's settlement increases compared with independent vertical loading (where  $T = 0$  N.m.) for the same vertical load. This confirms that the response of the pile to vertical loads under constant torsion loads is affected by the bigger torsion load. These results are consistent with Wang et al. (2020) and Zou et al. (2021).

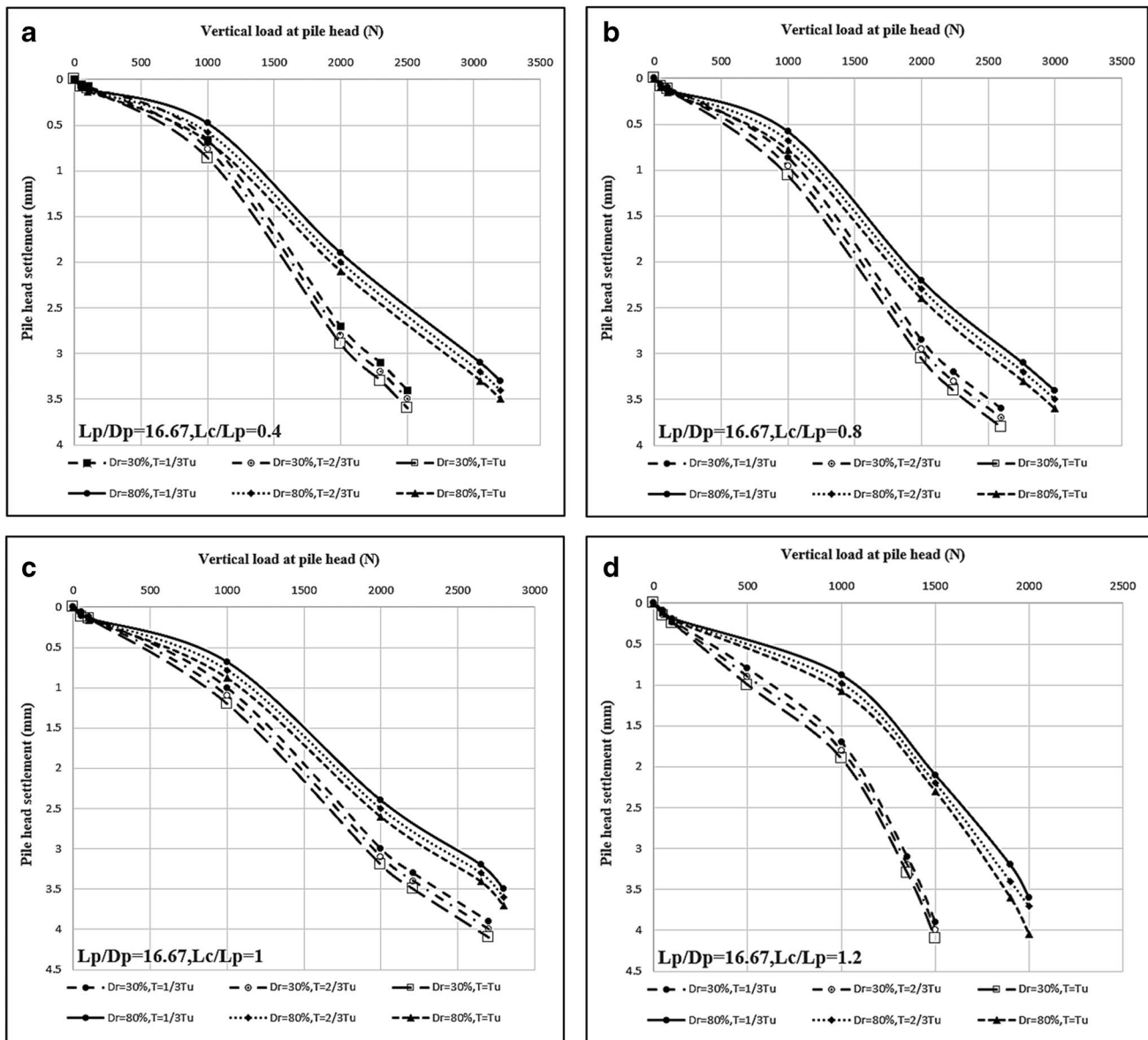


**Fig. 9** Relationship between the applied vertical load and settlement under pre-applied torsion load in contaminated sand, **a**  $L_c/L_p=0.4$ , **b**  $L_c/L_p=0.8$ , **c**  $L_c/L_p=1$ , **d**  $L_c/L_p=1.2$

**Influence of contaminated depth ( $L_c/L_p$ ) ratio**

The influence of the contaminated layers-to-embedded length ratio ( $L_c/L_p$ ) on the torsional capacity, vertical response, and combined load (pre-applied load) of the tested piles was investigated at various sand relative densities. Figure 12b shows how the contaminated layers-to-embedded length ratio ( $L_c/L_p$ ) affects pile behavior under vertical load when piles are installed in contaminated sand in the case of  $L_c/L_p=0.4, 0.8, 1,$  and  $1.2$  with a relative density of  $Dr=30$  and  $80\%$  and a stiffness ratio  $L_p/D_p=16.67$ . The vertical bearing capacity in contaminated sand at  $Dr=30\%$  was reduced by 9, 12, 14, and 42% compared to the vertical

bearing capacity in clean sandy soil at  $L_c/L_p=0.4, 0.8, 1,$  and  $1.2$ , respectively, while these values were decreased to reach 10, 19, 25, and 65% at  $Dr=80\%$  in that order. From the results, it is concluded that increasing the contaminated depth ( $L_c$ ) reduces the pile’s bearing capacity significantly. Nevertheless, it is demonstrated that raising  $L_c/L_p$  up to 0.8 has minimal effect on the pile’s toe-bearing capability. This might be attributed to the existence of clean sand surrounding the pile toe. The quantity of capacity is then dramatically lowered by raising the value of  $L_c/L_p$  until it reaches 1.2. This might be owing to the soil’s high compressibility in the presence of oil. This finding is in good support of the results of Ratnaweera and Meegoda (2006) and Nasr (2009).

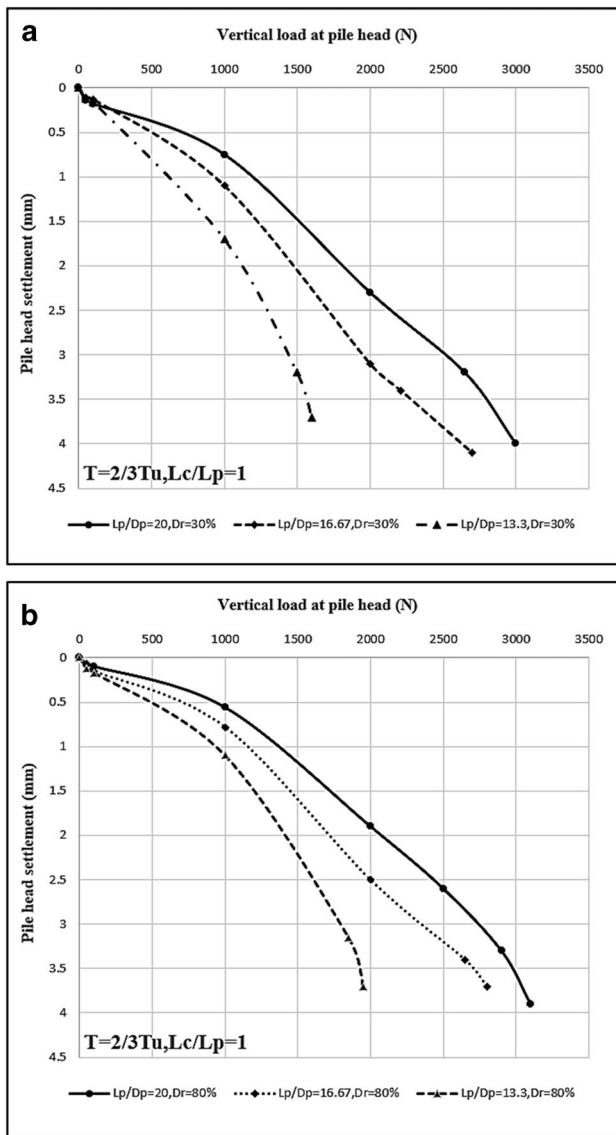


**Fig. 10** Applied vertical load and settlement relationship at  $L_c/L_p=1$  under pre-applied load ( $T=2/3T_u$ )

**Table 8** Maximum vertical load (N) obtained with and without constant torsional load,  $L_p/D_p=16.67$

Soil	$L_c/L_p$	$T=0$	$T=1/3T_u$	$T=2/3T_u$	$T=T_u$
Dr = 30%	0	2500	2471	2442	2413
	0.4	2300	2274	2247	2221
	0.8	2240	2214	2187	2161
	1	2210	2184	2158	2132
	1.2	1350	1324	1298	1272
Dr = 80%	0	3300	3268	3235	3203
	0.4	3050	3020	2990	2960
	0.8	2760	2731	2701	2672
	1	2650	2621	2592	2563
	1.2	1900	1871	1842	1813

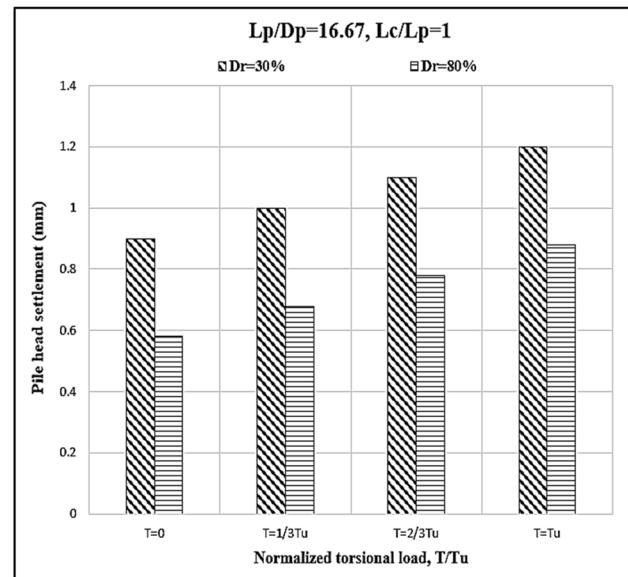


**Fig. 11** Settlement at normalized torsional loads ( $T/T_u$ ) and the same vertical load in contaminated loose and dense sand at  $L_p/D_p=16.67$  and  $L_c/L_p=1$

Figure 12a depicts the influence of contaminated layers on pile response to torsion load at  $Dr=30$  and  $80\%$  with  $L_p/D_p=16.67$  and  $L_c/L_p=0.4, 0.8,$  and  $1$ . The torsional capacity in contaminated sand at  $Dr=30\%$  was reduced by 8, 10, and 11% more than in clean sand at  $L_c/L_p=0.4, 0.8,$  and  $1$ , respectively. At  $Dr=80\%$ , these values were found to be 9, 11, and 12% lower than the torsional capacity in clean sandy soil at  $L_c/L_p=0.4, 0.8,$  and  $1$ , respectively. The findings of the experiments show that increasing the thickness of the contaminated sand layer has no discernible effect on the resultant torsion-bearing capacity. This is due to the influence of the top layer on torsion load, which is consistent with the findings of Zou et al. (2021). This is because the upper-layered soil qualities have the greatest impact on torsional resistance. It can be shown that increasing the thickness of the contaminated layers ( $L_c$ ) up to 0.4 has a substantial influence on the toe-bearing capabilities of the pile. When the  $L_c/L_p$  ratio was increased to 1, the toe capacity was a little changed. This demonstrates that the surrounding soil has a minor impact on the piles' bearing capability. This is consistent with the findings of Zou et al. (2020) and Zou et al. (2021). Based on this investigation, it can be stated that sand contaminated with oil has a lower torsional and vertical capacity of the piles than clean sand.

### Effect of pile stiffness ( $L_p/D_p$ )

According to previous works, one of the factors that determine pile resistance is the ratio of the depth of the pile embedded in the soil ( $L_p$ ) to the diameter ( $D_p$ ).

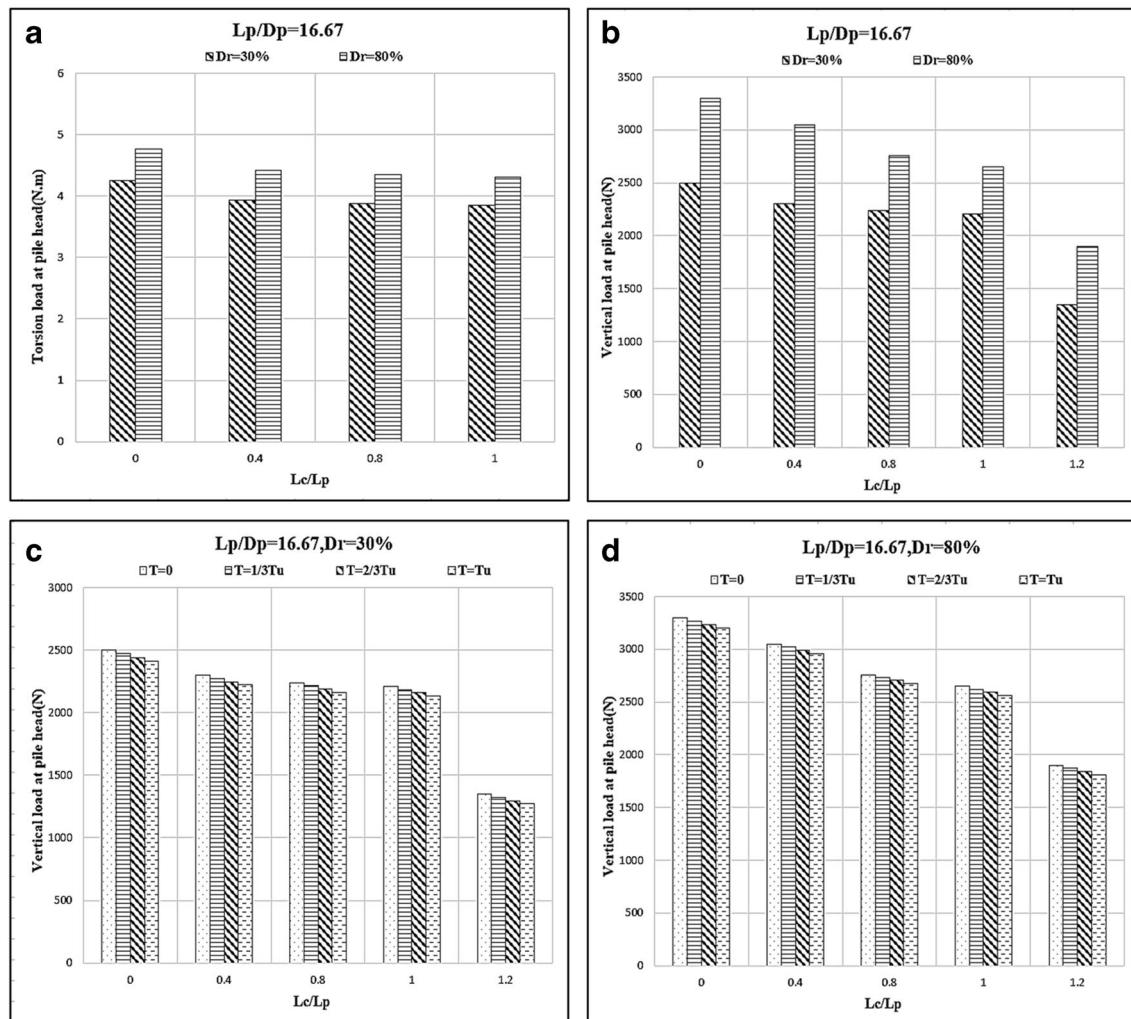


**Fig. 12** The influence of contaminated layers-to-embedded length ratio ( $L_c/L_p$ ) at  $L_p/D_p = 16.67$  of the pile **a**) Torsion load, **b**) Vertical load, **c**) combined load ( $T \rightarrow V$ ) in loose sand, **d**) combined load ( $T \rightarrow V$ ) in dense sand

In this study, the  $L_p/D_p$  ratio varied from 13.3 to 20. Increasing the embedded depth has a double influence on the pile’s bearing capacity by increasing the pile’s embedded surface area and the amount of stress at the pile. As illustrated in Fig. 13a, the impact of embedded length of pile-to-pile diameter ( $L_p/D_p$ ) on pile performance under vertical load in contaminated sand at  $D_r = 30$  and  $80\%$  with  $L_p/D_p = 20, 16.67,$  and  $13.3$  and  $L_c/L_p = 1$ . The vertical bearing capacity in contaminated sand at  $D_r = 30\%$  was found to be 2650, 2210, and 1500 N at  $L_p/D_p = 20, 16.67,$  and  $13.3,$  respectively, while at  $D_r = 80\%$ , these values were found to be 2900, 2650, and 1850 N in the case of  $L_p/D_p = 20, 16.67,$  and  $13.3,$  respectively, in that order. The results showed that the ultimate vertical pile resistance increased with an increase in the  $L_p/D_p$  ratio, indicating that a longer pile embedded in the soil provides greater resistance to loading. This analysis supports the results of Mohammadi et al. (2018). Figure 13b

illustrates the influences of the embedded length of pile-to-pile diameter ( $L_p/D_p$ ) on the behavior of piles under torsion load in contaminated sand at  $D_r = 30$  and  $80\%$  with  $L_p/D_p = 20, 16.67,$  and  $13.3$  and  $L_c/L_p = 1$ . The ultimate torsional capacity at  $D_r = 30\%$  in contaminated sand was 3.98, 3.85, and 3.73 N.m at  $L_p/D_p = 20, 16.67,$  and  $13.3,$  respectively, while these values at  $D_r = 80\%$  reached 4.48, 3.31, and 4.16 N.m, in the same order. It is demonstrated that increasing the value of the embedded length-to-pile diameter ratio ( $L_p/D_p$ ) improves the torsional bearing capacity of piles installed in contaminated sand. This supports the findings of Poulos (1975), Dutt and O’Neill (1983), Tawfiq (2000), and Zhang and Kong (2006). It should be observed that variations in  $L_p/D_p$  have a very sensitive influence on the pile’s torsional loading resistance. As can be seen, a change in pile length has a major influence on the piles’ capacity to withstand torsional loads. Furthermore, while the diameter of the

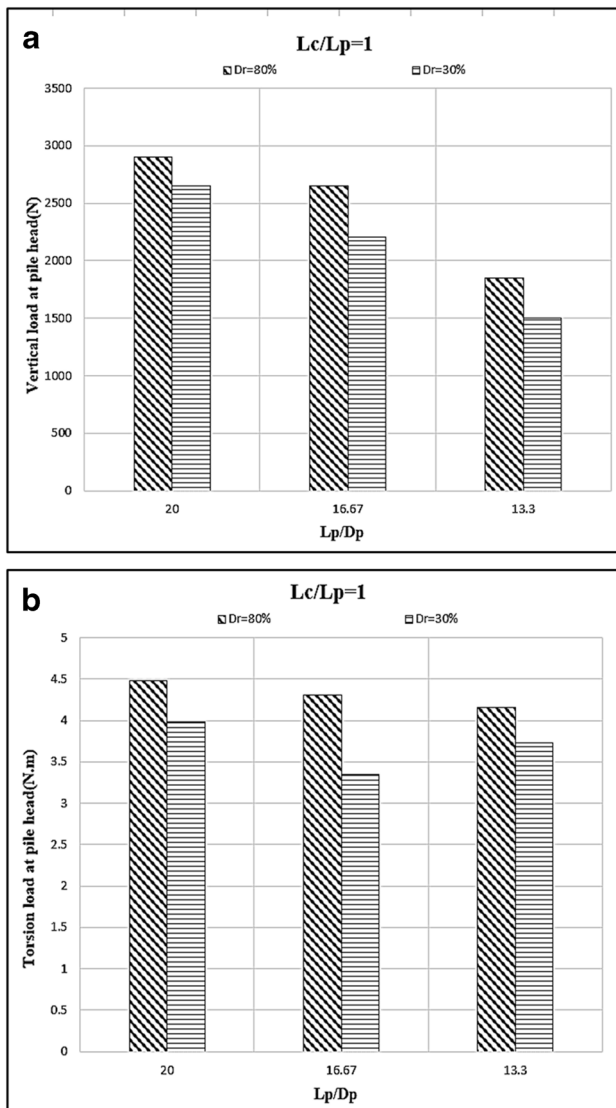


**Fig. 13** The influence of the embedded length of pile-to-pile diameter ( $L_p/D_p$ ) at  $L_c/L_p = 1$  under vertical and torsion load

piles remained constant, changing the length of the pile had a significant impact on the condition of piles installed in contaminated sandy soil. This indicates that the first layer which is 3 ~ 4 of the pile’s diameter ( $D_p$ ), determines the influence of a pile under torsional load.

**Influence of relative sand density  $Dr\%$**

The influence of relative densities ( $Dr\%$ ) on pile torsion capabilities at varying thinness ratios ( $L_p/D_p$ ) was examined. Figures 14 and 15 display the effect of relative densities ( $Dr\%$ ) on the influence of piles under torsion and a combined load of piles establishing into clean and contaminated sand at  $Dr = 30$

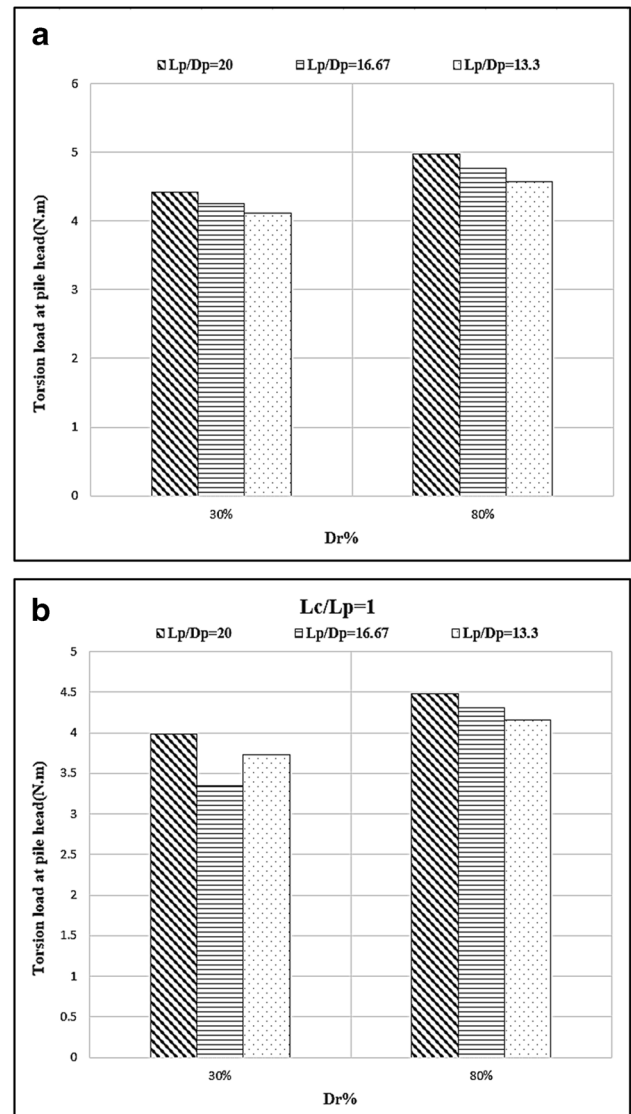


**Fig. 14** The effect of relative densities ( $Dr\%$ ) on the behavior of piles under torsion load in clean and contaminated sand

and 80% in the case of  $L_p/D_p = 20, 16.67, \text{ and } 13.3$  and  $L_c/L_p = 1$ . Figure 15 clarifies the vertical capacity under pre-applied load ( $T = 2/3 T_u$ ) in clean sand at  $Dr = 30\%$  was found to be decreased by 23, 32, and 33% compared with the piles at  $Dr = 80\%$ , in the case of  $L_p/D_p = 20, 16.67, \text{ and } 13.3$ , respectively, while these values in contaminated sand at  $Dr = 30\%$  were found to be decreased by 10, 22, and 24% compared with the piles at  $Dr = 80\%$ , in the cases of  $L_c/L_p = 1$ , and  $L_p/D_p = 20, 16.67, \text{ and } 13.3$ , respectively. Figure 14 explains the torsional capacity in clean sand at  $Dr = 30\%$  was found to be decreased by 11, 12, and 13% compared with the piles at  $Dr = 80\%$ , in the case of  $L_p/D_p = 20, 16.67, \text{ and } 13.3$ , respectively, while, these values in contaminated sand at  $Dr = 30\%$  were found to be decreased by 12, 13, and 14% compared with the piles at  $Dr = 80\%$ , in the cases of  $L_c/L_p = 1$  and  $L_p/D_p = 20, 16.67, \text{ and } 13.3$ , respectively.

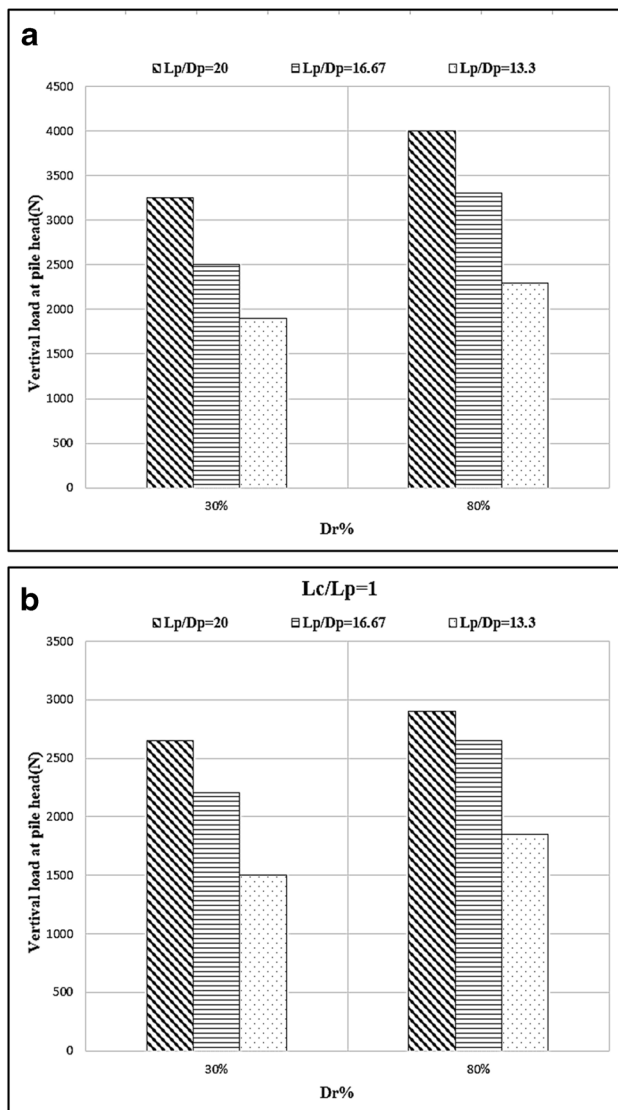


**Fig. 15** The effect of relative densities ( $Dr\%$ ) on the behavior of piles under pre-applied torsion load ( $T = 2/3T_u$ ) at  $L_c/L_p = 1$

$D_p = 20, 16.67,$  and  $13.3,$  respectively. As can be observed, increasing the relative density of sand ( $Dr\%$ ) from loose to dense increases the pile's torsional load capability. It was also discovered that when soil relative density increased, it also increased the amount of soil surrounding the pile. These findings can be attributed to a number of factors, including the following: first, when relative density increased, it correspondingly increased the horizontal subgrade response and the soil's relative stiffness ratio; second, dense soil particles moved more slowly than loose sand particles; third, the degree of particles interconnecting in dense sand is higher than in loose sand; and fourth, the soil volume around the pile was more responsive to soil relative density. These findings are consistent with those of Sabry (2001), McVay et al. (2003), Zhang and Kong (2006), and Nasr (2013). In accordance with the results of

oil-contaminated sand, the oil viscosity acts to lubricate the pile surface, and lubrication facilitates the smoothness of pile movement by reducing the angle of friction ( $\phi$ ). Oil contamination also caused a constant decrease in sand permeability. This is due to the fact that the presence of oil decreases the permeability coefficient of the sand as well as the volume of soil porosity. According to this data, it was concluded that increasing the relative density of the sand will result in improved results when installing piles in oil-contaminated sand.

### Rotation and torsion along the pile

In the current investigation, the values of torsion and twist angle along the pile may be calculated using Eqs. 1 and 2. Figure 16 expresses the torque along the pile of piles installed in oil-contaminated sand in the case of  $L_p/D_p = 16.67$  and  $L_c/L_p = 1$ . At relative densities ( $Dr = 30$  and  $80\%$ ), the toe resistance contributed around 31% and 39% of the torsional resistance, respectively. The findings show that the curves for loose sand have slopes that were the highest in the intermediate depths but progressively reduced approaching the pile toe, whereas the curves for dense sand grow continuously with increased loads. This agrees with the findings of Zhang and Kong (2006) and Zou et al. (2021). Figure 17 shows the rotation along the pile length of piles installed in clean and contaminated sand at  $Dr = 30$  and  $80\%$  in the cases of  $L_p/D_p = 16.67$  and  $L_c/L_p = 0.4, 0.8,$  and  $1,$  respectively. As can be seen in the clean condition, the rotation approaches zero at a depth of  $0.6 L$  (this depth is known as the critical depth), but in the contaminated condition, this value is obtained at a depth of  $0.8 L$  for a totally contaminated depth. However, this value was observed to range from  $0.65$  to  $0.75$  at partly contaminated depth. Therefore, it is important to carefully consider the critical depth when designing deep foundations to ensure stability and prevent excessive soil pressure that could lead to structural failure. Additionally, appropriate measures such as reinforcement or soil improvement techniques may need to be implemented to mitigate the effects of high soil pressure.

### Scale and boundary effects' influence

Laboratory tests are extensively used on small paradigms because of the high time and money costs for field testing as well as the numerous construction, equipment, and loading requirements. According to Muir Wood 2004, the main cause of these variations is the stress that field tests and laboratory tests experience under different conditions. which the stress surrounding the models is lower than in full-size models. Model piles were used to study the impact of piles on torsional capacity with nearly the same pile diameter ( $D_p$ ) but different lengths ( $L_p$ ). The

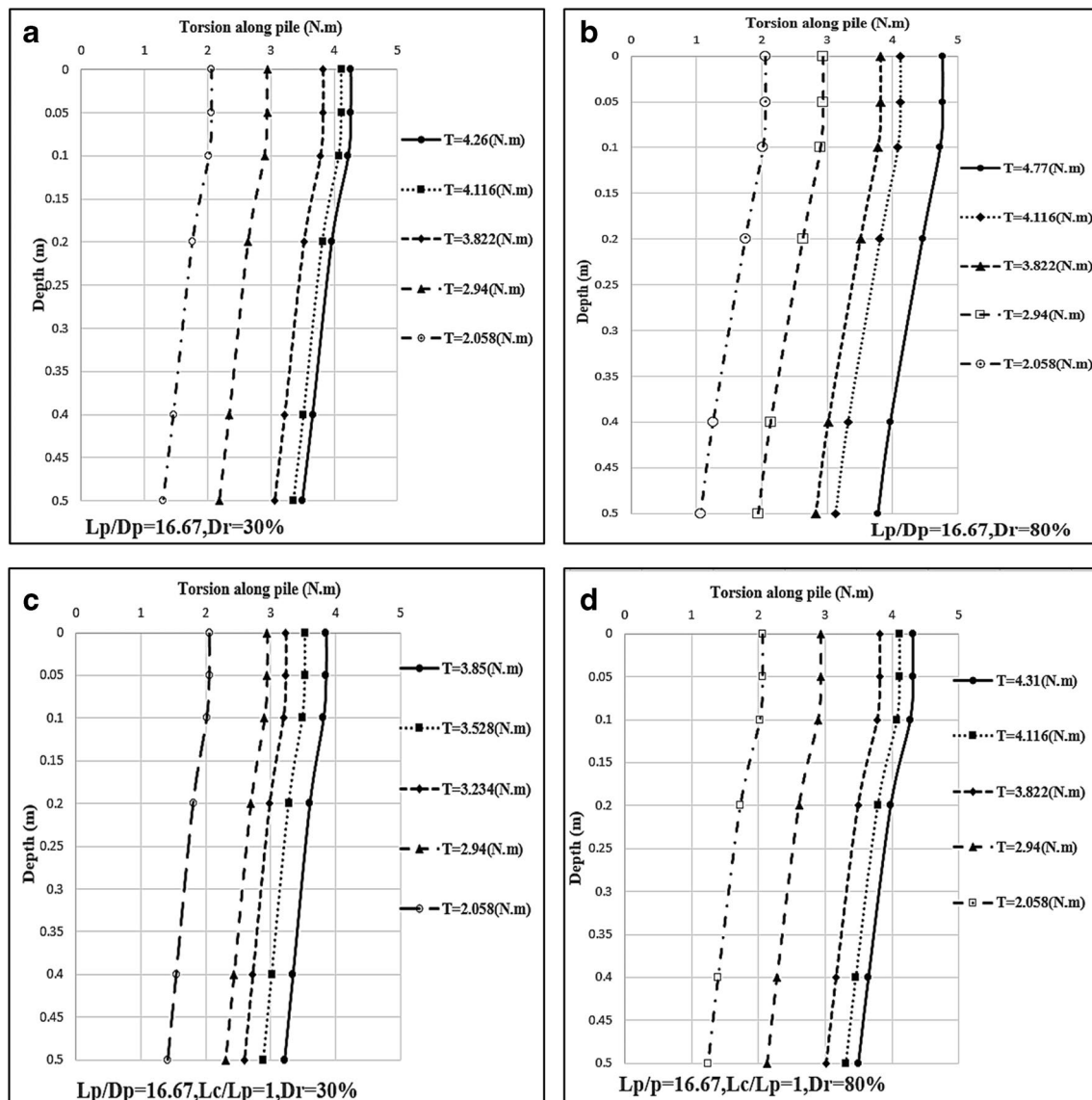


**Fig. 16** Transfer of torque along the pile at  $L_p/D_p=16.67, L_c/L_p=1$  in loose and dense sand

minimum pile diameter was chosen at 30 mm, which is comparable to the Vesic (1977) standard for a minimum pile size of 30 mm. The sand grain size distribution employed in this study was selected to prevent the scale of particle size inaccuracy (Franke and Muth 1985; Basha and Azzam 2018; Sakr et al 2020) by having a ratio of pile diameter ( $D_p$ ) to mean grain size of sand ( $D_{50}$ ) greater than 30. In a large tank, piles were tested to eliminate boundary effects. One of the most crucial elements affecting the correct interaction of the soil is the consistent size of the shear band next to the pile. According to Boulon and Foray (1986), the shear band's thickness, which is typically about 10  $D_{50}$ , depends on the relationship between the pile's coarseness and the ratio between the size of the grains in  $D_{50}$ . In current tests, the ratio of pile diameter to

average grain size ( $D_{50}$ ) must be greater than 35 for vertical substrate loading and greater than 44 for lateral loads (Balachowski (2006) and Azzam and Elwakil (2016)). The percentage reduces by roughly 3–5% in field testing; however, it is more noticeable for tiny laboratory models than for full-size field models.

## Conclusions

This study investigated how contamination with oil affected the ability of piles to support torsional loads ( $T$ ) and combined loads ( $T \rightarrow V$ ). In order to simulate the impact of torsional stresses on a pile's capacity, this research provided a number of small experiments. Changes were made to the

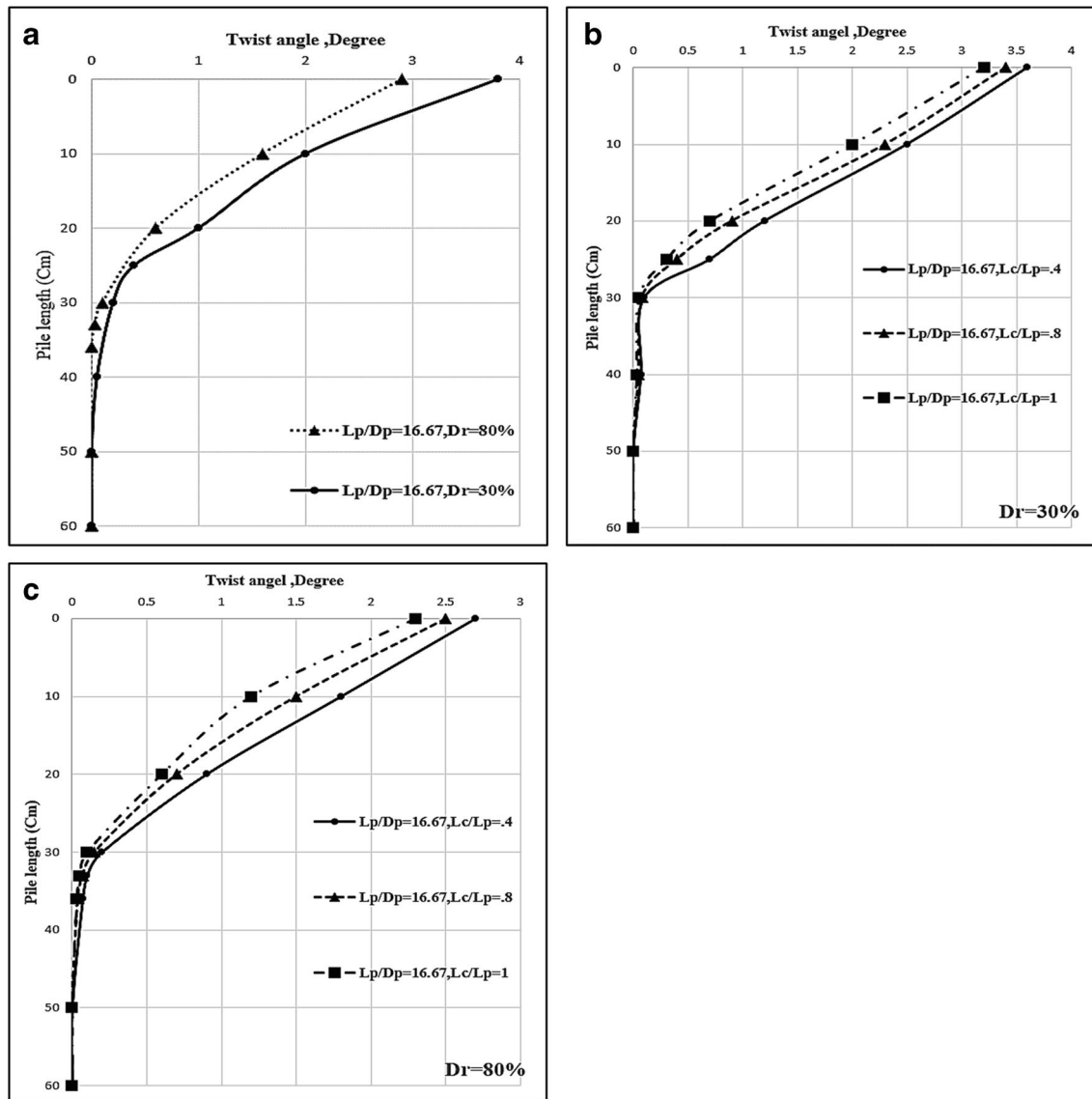


Fig. 17 Torsion angle in both clean and contaminated sand at  $L_p/D_p = 16.67$  along the length of the pile

relative densities of the sand ( $D_r\%$ ), the thickness of the contaminated layer ( $L_c$ ), and the length embedded in the sand soil ( $L_p$ ) in order to conduct the experiments. The conclusions based on the findings were summed up as follows:

- (1) In dense sand, at  $L_p/D_p = 20$  and  $L_c/L_p = 1$ , the torsional bearing ability of the pile in oil-contaminated sand at  $1^\circ$  is found to be 33% of the maximum torsional load, while this value is found to be 29, and 32% in the case of  $L_c/L_p = 0.33$ , and  $0.67$  respectively.
- (2) The ultimate vertical capacities of piles in oil-contaminated sand under pre-loading ( $T = 2/3T_u$ ) were reduced by 3.8, 4.1, and 4.5% compared with the pile under independent vertical load for the cases of  $L_p/D_p = 20, 16.67,$  and  $13.3$  and  $L_c/L_p = 1, 0.75,$  and  $0.5$ , respectively.

- (3) The ultimate vertical capacities of piles in oil-contaminated sand under pre-loading at  $T = 2/3T_u$  were decreased by 2, 1.5, and 1.8% compared to the pile under pre-loading at  $T = 1/3T_u$  for the cases of  $L_p/D_p = 20, 16.67,$  and  $13.3$  and  $L_c/L_p = 1$ , respectively, in loose sand.
- (4) In the cases of  $L_p/D_p = 20, 16.67,$  and  $13.3,$   $L_c/L_p = 1,$  and  $D_r = 80\%$ , while at constant torsional load  $T = 2/3T_u$  and the same vertical load, the settlement was increased by 57, 35, and 20% more than the settlement at no torsional load ( $T = 0$  N.m.).
- (5) For the cases of  $L_p/D_p = 20, L_c/L_p = 0.33, 0.67,$  and  $1,$  and  $D_r = 30\%$ , the torsional capacities of piles in contam-

inated sand were reduced by 9, 10, and 11% compared to the torsional capabilities of piles in clean sand.

- (6) Increasing the thickness of the contaminated layer ratio ( $L_c/L_p$ ) up to 0.4 will lead to a significant decrease in the torsional load-bearing capacity of the piles. In contrast to the vertical load, increasing  $L_c/L_p > 0.4$  led to a marked decrease in the bearing capacity of the pile.
- (7) The torsional capacity of piles is significantly influenced by the properties of the upper-layered soil; hence, an increase in the thickness of the contaminated sand layer has a negligible impact on this capacity.
- (8) The pile failure happens at a small twist angle for piles installed in oil-contaminated sand because the oil viscosity acts to lubricate the pile surface, and lubrication enhances the smoothness of pile movement by reducing the angle of friction ( $\phi$ ), causing the pile to slip suddenly.
- (9) The behavior of loose and dense sand under pile torsion loading is significantly different and should be considered when designing foundations for structures.
- (10) It is important to consider the critical depth when designing pile foundations to ensure stability and minimize soil pressure. Additionally, measures such as increasing the pile diameter or adding reinforcement can be taken to reduce displacement and angle of torsion in cases where  $L/Z$  is less than 0.6.

**Data availability** Not applicable.

## Declarations

**Ethics approval** This research did not contain any studies involving animal or human participants, nor did it take place in any private or protected areas. No specific permissions were required for corresponding locations.

**Consent to participate** All authors agree to participate.

**Consent for publication** All authors agree to publish this manuscript.

**Conflict of interest** The authors declare no competing interests.

## References

- Abdelhalim R et al (2020) Experimental and numerical studies of laterally loaded piles located near oil-contaminated sand slope. *Eng Sci Technology, An Int J*. <https://doi.org/10.1016/j.jestch.2020.03.001>
- ASTM (2010) ASTM D2487: Standard practice for classification of soils for engineering purposes (Unified Soil Classification System). ASTM International, West Conshohocken, PA, USA
- Azzam WR (2015) Utilization of the confined cell for improving the machine foundation behavior. *J GeoEng* 10(1):17–23
- Azzam W, Elwakil A (2016) Performance of axially loaded-piled retaining wall: experimental and numerical analysis. *Int J Geomech*. [https://doi.org/10.1061/\(ASCE\)GM.1943-5622.0000710.04016049](https://doi.org/10.1061/(ASCE)GM.1943-5622.0000710.04016049)
- Balachowski L (2006) Scale effect in shaft friction from the direct shear interface tests. *Arch Civ Mech Eng* 4(3):14–29
- Basack S et al (2011) An analytical solution for single pile subjected to torsion. In: Proceedings of Indian geotechnical conference December 15–17, 2011, Kochi (N-016)
- Basack S, Nimbalkar S (2017) Numerical solution of single pile subjected to torsional cyclic load. *Int J Geomech* 17(8):04017016. [https://doi.org/10.1061/\(ASCE\)GM.1943-5622.00009095](https://doi.org/10.1061/(ASCE)GM.1943-5622.00009095)
- Basack S, Sen S (2014) Numerical solution of single piles subjected to pure torsion. *J Geotech Geoenviron Eng* 140(1):74–90. [https://doi.org/10.1061/\(ASCE\)GT.1943-5606.0000964](https://doi.org/10.1061/(ASCE)GT.1943-5606.0000964)
- Basha A, Azzam W (2018) Uplift capacity of single pile embedded in partially submerged sand. *KSCE J Civ Eng* 22(12):4882–4890
- Bizaliele MM (1992) Torsional cyclic loading response of a single pile in sand. In: Dissertation, presented to Schriftenreihe des Instituts für Grundbau. Ruhr-Univ, Bochum
- Bolton MD et al (1999) Centrifuge cone penetration tests in sand. *Geotechnique* 49(4):543–552. <https://doi.org/10.1680/geot.1999.49.4.543>
- Boulon M, Foray P (1986) Physical and numerical simulation of lateral shaft friction along offshore piles in sand. In: Third international conference on numerical methods in offshore piling, Nantes, pp 127–147
- Chow YK (1985) Torsional response of piles in nonhomogeneous soil. *J Geotech Eng* 111(7):942–947. [https://doi.org/10.1061/\(ASCE\)0733-9410\(1985\)111:7\(942\)](https://doi.org/10.1061/(ASCE)0733-9410(1985)111:7(942))
- Craig WH, Sabagh SK (1994) Stress-level effects in model tests on piles. *Can Geotech J* 31(1):28–41. <https://doi.org/10.1139/t94-004>
- Dhatrak A, Sabale S, Thakare S (2017) Performance of single pile in oil contaminated sand under axial loading. *Int J Eng Sci Res Technol*. <https://doi.org/10.5281/zenodo.817966>
- Dutt RN, O'Neill MW (1983) Torsional behavior of model piles in sand. In: Wright SG (ed) *Geotechnical practice in offshore engineering*. American Society of Civil Engineers, New York, NY, USA, pp 315–334
- Dutt RN (1976) Torsional response of piles in sand. PhD thesis, University of Houston, Houston, TX, USA, 7 115–123
- Franke E, Muth G (1985) Scale effect in 1g model tests on horizontally loaded piles. In: Proceedings of the 11th International Conference on Soil Mechanics and Foundation Engineering, vol 2, San Francisco, pp 1011–1014
- Garnier J et al (2007) Catalogue of scaling laws and similitude questions in geotechnical centrifuge modeling. *Int J Phys Model Geotech* 7(3):1–23. <https://doi.org/10.1680/ijpimg.2007.070301>
- Garnier J, Konig D (1998) Scale effects in piles and nails loading tests in sand. In: Proc., Centrifuge'98, Vol. 1, Tokyo, pp 205–e210
- Garnier J (2001) Physical models in geotechnics: State of the art and recent advances, 1st Coulomb lecture, Paris
- Georgiadis M, Saflekou S (1990) Piles under axial and torsional loads. *Comput Geotech* 9(4):291–305. [https://doi.org/10.1016/0266-352X\(90\)90043-U](https://doi.org/10.1016/0266-352X(90)90043-U)
- Guo WD (2000) Vertically loaded single piles in Gibson soil. *J Geotech Geoenviron Eng* 126(2):189–1930. [https://doi.org/10.1061/\(ASCE\)1090-0241\(2000\)126:2\(189\)](https://doi.org/10.1061/(ASCE)1090-0241(2000)126:2(189))
- Guo WD, Randolph MF (1997) Vertically loaded piles in non-homogeneous media. *Int J Numer Analyt Methods Geomech* 21(8):507–532. [https://doi.org/10.1002/\(SICI\)1096-9853\(199708\)21:8%3c507::AID-NAG888%3e3.0.CO;2-V](https://doi.org/10.1002/(SICI)1096-9853(199708)21:8%3c507::AID-NAG888%3e3.0.CO;2-V)
- Guo P, Zou X (2018) Bearing capacity of a single pile in sand under combined vertical force-horizontal force-torque load. *Chin J Rock Mech Eng* 31(11):2593–2600 (in Chinese)

- Khamehchiyan M, Charkhabi AH, Tajik M (2007) Effects of crude oil contamination on geotechnical properties of clayey and sandy soils. *Eng Geol* 89:220–229
- Laue J, Sonntag T (1998) Pile subjected to torsion. In: Proceedings of centrifuge '98, Balkema, Rotterdam, the Netherlands, pp 187–192
- Leblanc C, Houlsby GT, Byrne BW (2010) Response of stiff piles in sand to long-term cyclic lateral loading. *Géotechnique* 60(2):79–90. <https://doi.org/10.1680/geot.7.00196>
- Li Q, Stuedlein AW (2018) Simulation of torsionally-loaded deep foundations considering state-dependent load transfer. *J Geotech Geoenviron Eng* 144(8):0401805. [https://doi.org/10.1061/\(ASCE\)GT.1943-5606.0001930](https://doi.org/10.1061/(ASCE)GT.1943-5606.0001930)
- Li Q, Stuedlein AW, Barbosa AR (2017) Torsional load transferred of drilled shaft foundations. *J Geotech Geoenviron Eng* 143(8):725–735. [https://doi.org/10.1061/\(ASCE\)GT.1943-5606.0001701](https://doi.org/10.1061/(ASCE)GT.1943-5606.0001701)
- McVay MC, Hu Z (2003a) Determine optimum depths of drilled shafts subject to combined torsion and lateral loads from centrifuge testing (using KB polymer slurry)-supplemental research. In: Report no. BC-545, WO #4. Florida Department of Transportation, Tallahassee, FL
- McVay MC, Herrera R, Hu Z (2003b) Determine optimum depths of drilled shafts subject to combined torsion and lateral loads using centrifuge testing. Rep. contract no. BC-354, RPWO #9
- McVay MC, Bloomquist D, Thiyyakkandi S (2014) Field testing of jet-grouted piles and drilled shafts. Report BDK75-977-41, 91977. Florida Department of Transportation, Tallahassee
- Mohammadi A et al (2018) Axial compressive bearing capacity of piles in oil-contaminated sandy soil using FCV. *Mar Georesources Geotechnol*. <https://doi.org/10.1080/1064119X.2017.1414904>
- Muir Wood D (2004) *Geotechnical modelling*. Spon Press, London, UK
- Nabil FI (2001) Axial load tests on bored piles and pile groups in cemented sands. *J Geotech Geoenviron Eng* 127(9):766–773
- Nasr AMA (2009) Experimental and theoretical studies for the behavior of strip footing on oil-contaminated sand. *J Geotech Geoenviron Eng* ASCE 135(12):1814–1822
- Nasr A (2013) Uplift behavior of vertical piles embedded in oil-contaminated sand. *J Geotechn Geoenviron Eng*. [https://doi.org/10.1061/\(ASCE\)GT.1943-5606.0000739](https://doi.org/10.1061/(ASCE)GT.1943-5606.0000739)
- Nasr A (2014) Experimental and theoretical studies of laterally loaded finned piles in sand. *Can Geotech J* 51:381–393
- Nasr A, Krishna Rao S (2016) “Behaviour of laterally loaded pile groups embedded in oil-contaminated sand”, *Géotechnique* 66(1):58–70. <https://doi.org/10.1680/jgeot.15.P.076>
- Nasr AAM, Azzam W (2017) Behaviour of eccentrically loaded strip footings resting on sand. *Int J Phys Model Geotech*. <https://doi.org/10.1680/jphmg.16.00008>
- Nghiem HM, Chang NY (2019) Pile under torque in nonlinear soils and soil-pile interface. *Soils Found* published online. <https://doi.org/10.1016/j.sandf.2019.08.012>
- Poulos HG (1975) Torsional response of piles. *J Geotech Eng Div* 101(10):1019–1035. <https://doi.org/10.1061/AJGEB6.0000203>
- Poulos HG, Davis EH (1968) The settlement behaviour of single axially-loaded incompressible pile and piers. *Géotechnique* 18(3):351–371. <https://doi.org/10.1680/geot.1968.18.3.351>
- Poulos HG, Davis EH (1980) Pile foundation analysis and design. In: Rainbow bridge book. University of Sydney
- Randolph MF (1983) Design consideration for offshore piles. *Geotechnical Practices in Offshore Engineering*, ASCE, Austin., pp. 422–439. [https://doi.org/10.1016/0148-9062\(85\)92244-2](https://doi.org/10.1016/0148-9062(85)92244-2)
- Ratnaweera P, Meegoda JN (2006) Shear strength and stress-strain behavior of contaminated soils. *Geotech Test J* 29(2):1–8
- Reddy KM, Ayothiraman R (2015) Experimental studies on behaviour of single pile under combined uplift and lateral loading. *J Geotech Geoenviron Eng* 141(7):04015030
- Sabry M (2001) Shaft resistance of a single vertical or batter pile in sand subjected to axial compression or uplift loading. M.Sc. thesis. Concordia Univ, Montréal
- Sakr M, Nazir AK, Azzam WR, Sallam A (2016) Behavior of grouted single screw piles under inclined tensile loads in sand. *Electron J Geotech Eng (EJGE)* 21:571–591
- Sakr M, Nazir AK, Azzam WR, Sallam A (2020) Model study of single pile with wings under uplift loads. *Appl Ocean Res* 100(102187):1–17
- Stoll UW (1972) Torque shear test of cylindrical friction piles. *J Civ Eng* 42(4):63–65
- Tawfiq K (2000) Drilled shafts under torsional loading conditions. Florida Department of Transportation, Tallahassee Report No. B-9191. <https://trid.trb.org/view.aspx?id=655455>
- Thiyyakkandi S, McVay MC, Lai P, Herrera R (2016) Full-scale coupled torsion and lateral response of mast arm drilled shaft foundations. *Can Geotech J* 53(12):1928–1938. <https://doi.org/10.1139/cgj-2016-0241>
- Vesic AS (1977) Design of pile foundation. National cooperative highway research program. In: Synthesis of Highway practice no. 42, Transportation Research Board, Washington
- Wang WS, Jiang J, Fu ZC, Ou DX, Tang J (2020) Analysis of the bearing characteristics of single piles under vertical and torsional combined loads. *J Hindawi*. <https://doi.org/10.1155/2021/8896673>
- Zhang LM, Kong LG (2006) Centrifuge modeling of torsional response of piles in sand. *Can Geotech J* 43(5):500–515. <https://doi.org/10.1139/t06-020>
- Zou XI, Zhou CH, Wang YI (2021) Experimental studies on the behaviour of single pile under combined vertical-torsional loads in layered soil. *J Appl Ocean Res*. <https://doi.org/10.1016/j.apor.2020.102457>
- Zou X, Zhao L, Zhou M, Tian Y (2020) Investigation of the torsional behaviour of circular piles in doublelayered nonhomogeneous soil. *Applied Ocean Res*. <https://doi.org/10.1016/j.apor.2020.102110>

Springer Nature or its licensor (e.g. a society or other partner) holds exclusive rights to this article under a publishing agreement with the author(s) or other rightsholder(s); author self-archiving of the accepted manuscript version of this article is solely governed by the terms of such publishing agreement and applicable law.